Available online at www.sciencedirect.com
SCIENCE DIRECT®
Solid State Ionics 159 (2003) 35–47
SOLID STATE IONICS
www.elsevier.com/locate/ssi

$Na_3Al_2(PO_4)_3$, a fast sodium conductor at high pressure: in-situ impedance spectroscopy characterisation and phase diagram up to 8 GPa

Fabrice Brunet[a,*], Nikolai Bagdassarov[b], Ronald Miletich[c]

[a] *Laboratoire de Géologie, CNRS-UMR 8538, Ecole Normale Supérieure, 24 rue de Lhomond, F-75231 Paris Cedex 5, France*
[b] *Institut für Meteorologie und Geophysik, Universität Frankfurt, Frankfurt am Main, Germany*
[c] *Laboratorium für Kristallographie, ETH-Zentrum, Zürich, Switzerland*

Received 18 November 2002; accepted 19 December 2002

Abstract

Solid-state syntheses on the $Na_3Al_2(PO_4)_3$ composition have been carried out from 850 to 1273 K at pressures up to 8 GPa. At 923 K and pressures above ca. 0.5 GPa, $Na_3Al_2(PO_4)_3$ crystallises in a NASICON-type structure and becomes an ionic conductor with a bulk conductivity of around 5.10^{-2} S/cm at 600 K, 1.5 GPa. Actually, the form recovered at room conditions is the monoclinic deformation of the rhombohedral NASICON cell. The two non-quenchable phase-transitions which lead to the true *R*-3*c* NASICON cell are met in high-pressure impedance spectroscopy (HPIS) experiments at 410 and 451 K, 0.4 GPa, and 454 and 508 K, 1.5 GPa, respectively. At 1073 K and pressures of 3.9, 6 and 8 GPa, another $Na_3Al_2(PO_4)_3$ form is obtained which is isostructural to rhombohedral $Na_3Fe_2(AsO_4)_3$ (II-NaFeAs), the high-temperature modification of $Na_3Fe_2(AsO_4)_3$ garnet (I-NaFeAs). A third $Na_3Al_2(PO_4)_3$ form of unknown structure is recovered in the lowest pressure syntheses, which displays a relatively low bulk conductivity comprised, at 0.3 GPa, between 5×10^{-4} S/cm at 900 K and 5×10^{-6} S/cm at 600 K. The effect of pressure is to stabilise the NASICON structure for a compound with relatively small cations (Na, Al, P). In addition, high pressures allow a transition from the NASICON structure to the II-NaFeAs structure, which had never been obtained under the sole effect of temperature at ambient pressure.

PACS: 66.30.Hs; 64.70.Kb; 81.30.Dz
Keywords: NASICON; Fast Na-conductivity; High-pressure impedance spectroscopy; Phase transition

1. Introduction

Amorphous $Na_3Al_2(PO_4)_3$ has been recently recognised to belong to the vast family of solid ionic conductors referred in the literature to as NASICON [1,2]. The high sodium-conductivity and the good cation-exchange properties of the members of NASICON-structure compounds such as $Na_{1+x}Zr_2Si_xP_{3-x}O_{12}$ series with $0<x<3$ (traditional NASICON series [3,4]), or new series like $Na_{1+x}Ti_{2-x}Al_x(PO_4)_3$ with $0<x<0.9$ [5] and $Na_3V_2(PO_4)_3$ [6], as well as a growing potential application of them in battery

* Corresponding author. Tel.: +33-1-44322274; fax: +33-1-44322000.
E-mail address: Brunet@geologie.ens.fr (F. Brunet).

0167-2738/03/$ - see front matter © 2003 Elsevier Science B.V. All rights reserved.
doi:10.1016/S0167-2738(03)00005-5

electrodes and for chemical sensors, have motivated recent studies of structurally related compounds. For example, most compounds with a general formula $Me^{+}_{3}(Me^{3+})_2(Me^{5+}O_4)_3$ (with Me^{+} = Na, Li, Ag or K, Me^{3+} = Ga, Cr, Fe, Al, Sc or In and Me^{5+} = As or P) belong to the NASICON-class where the mechanism of the electrical conductivity infers hopping of Na ions among adjacent sites M(1), M(2) and M(3) through channels parallel to the *c*-axis built in the anionic framework of $Me^{3+}O_6$ octahedra and $Me^{5+}O_4$ tetrahedra [3,7]. Besides the fast ionic conductivity, some of these compounds of NASICON-structure possess a low thermal expansion [8,9]. They can also be potentially used as sensors for some ion-exchange and redox insertion/extraction reactions under mild experimental conditions [6]. The sodium phosphates, $Na_3(Me^{3+})_2(PO_4)_3$ (with Me^{3+} = Fe, Cr, In, Sc), crystallise with the true *R*-3*c* $NaZr_2(PO_4)_3$ structure, first established in Ref. [10], and they all show similar structural properties [11]. Apart from $Na_3In_2(PO_4)_3$, all these phosphates display a monoclinic modification towards low temperatures [11–14], similar to that described in Ref. [15] for $Na_3Zr_2Si_2PO_{12}$ NASICON. Sodium arsenates, structurally related compounds, were less studied than their phosphate analogues. Sodium arsenates, with Me^{3+} = Cr and Fe, adopt the garnet structure [16] and show a high-temperature rhombohedral modification with an open structure, called II-NaFeAs [17]. Sodium arsenates with a smaller trivalent cation (Me^{3+}), like Al and Ga, are only known under the II-NaFeAs form. When, on the contrary, larger cations like Sc or In are incorporated, then $Na_3Sc_2(AsO_4)_3$ crystallises with the true *R*-3*c* NASICON structure whereas $Na_3In_2(AsO_4)_3$ crystallises into a fourth, alluaudite-like, structure [18]. Besides that, the substitution of Li for Na in $Na_3Fe_2(AsO_4)_3$ stabilises the garnet structure [19].

The structures which were under the scope of previous 1-bar studies for $Na_3(Me^{3+})_2(PO_4)_3$ and $Na_3(Me^{3+})_2(AsO_4)_3$, with Me^{3+} = Al, Fe, Cr, Sc,

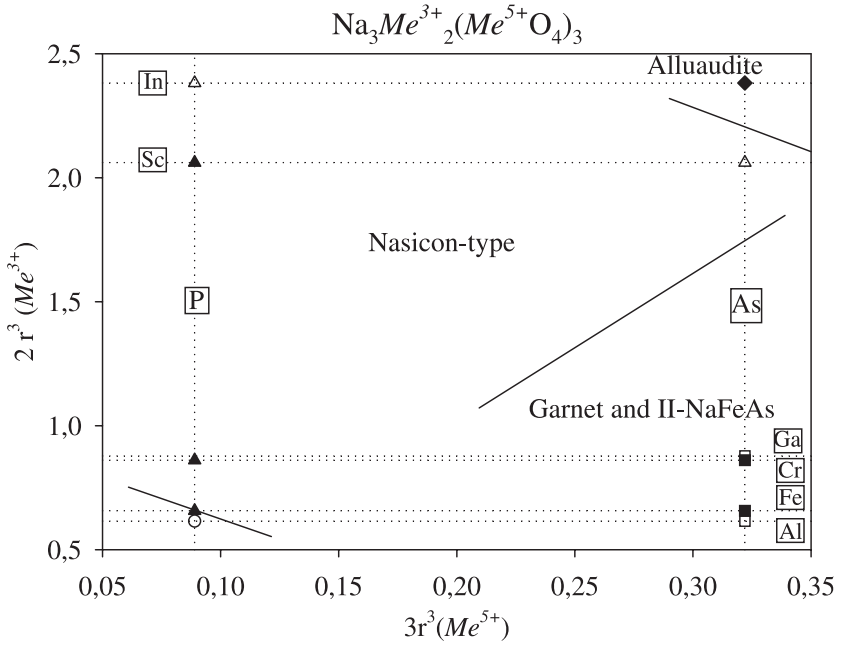

Fig. 1. Structures of $Na_3(Me^{3+})_2(Me^{5+}O_4)_3$ with Me^{3+} = Al, Fe, Cr, Sc, In, and Me^{5+} = As and P located in the space of the Me^{3+} and Me^{5+} cation volume (ionic radii are taken from Ref. [20]). Alluaudite (solid diamond), NASICON without low-temperature modifications (empty triangle), NASICON with low-temperature modifications (solid triangles), $Na_3Fe_2(AsO_4)_3$ structure without garnet modification (empty squares), $Na_3Fe_2(AsO_4)_3$ structure with garnet modification (solid squares). Empty circle corresponds to the plot of the $Na_3Al_2(PO_4)_3$ composition.

and In, are reported in a two-dimensional space of both pentavalent (As and P) and trivalent (Me^{3+}) cation ionic volume (Fig. 1). Three types of structures can be defined. The NASICON-type structure field includes phases with the $NaZr_2(PO_4)_3$ structure with or without monoclinic modification. It is a wide field including all phosphate as well as scandium arsenate compositions. Most arsenates, however, crystallise with the rhombohedral II-NaFeAs structure (with or without garnet modification, I-NaFeAs). At one end of the diagram (Fig. 1), $Na_3In_2(AsO_4)_3$ corresponds to the compositions with the largest cations; $Na_3In_2(AsO_4)_3$ crystallises with the alluaudite structure. At the opposite end, $Na_3Al_2(PO_4)_3$ with the smallest cations has never been obtained from dry synthesis [15]. It must be noted that temperature does not affect the boundary between the various structure fields. In other words, polymorphic relationships have never been described at atmospheric pressure between the structures mentioned in Fig. 1. Actually, this does not hold true for the $NaCa_2Me^{2+}{}_2(AsO_4)_3$ compounds (with Me^{2+} = Mg, Ni, Co) which exhibit a garnet–alluaudite transition [21]. It has been claimed in Ref. [22] that the synthesis of $Na_3Al_2(PO_4)_3$ garnet could be achieved by cooling a molten $Na_3PO_4 + AlPO_4$ mixture at ambient pressure. However, the inspection of Fig. 1 shows that the growth of $Na_3Al_2(PO_4)_3$ garnet at ambient pressure is unlikely. As a matter of fact, the garnet structure has been recognised in arsenate compounds but never in their phosphate counterparts in relation to the smaller size of the P^{5+} ion. Previous studies dealing with $Na_3(Me^{3+})_2(Me^{5+}O_4)_3$ compounds were undertaken at atmospheric pressure. They mainly aimed at producing, by varying both temperature and cation size, NASICON compounds with various structural opening. Due to the small size of the Me^{3+} and Me^{5+} cations in $Na_3Al_2(PO_4)_3$, pressure appears to be a key parameter to obtain the *R*-3*c* NASICON structure, which is commonly found for $Na_3(Me^{3+})_2(Me^{5+}O_4)_3$ compounds. It can be mentioned at this stage that the Na^+ conductivity in $Na_3Al_2(PO_4)_3$ is expected to be comparatively low and the activation energy to be high in a NASICON framework composed by a small octahedral metal like Al^{3+} [9]. The ionic conductivity of crystalline $Na_3Al_2(PO_4)_3$ has never been investigated, however, and is the focus of this study.

2. Experimental

2.1. Syntheses

The 3/2 $Na_2O + Al_2O_3 + 3/2\ P_2O_5$ stoichiometry is achieved by grinding under ethanol a mixture of $Na_2CO_3 + Al_2O_3 + NH_4H_2PO_4$ (Aldrich©, 99.999%) in an agate mortar. The homogeneous mixture is then held for 1 h at 873 K and for another hour at 1273 K and then quenched in air. A recrystallised melt has been recovered, then it was crunched into millimeter-sized pieces and subsequently milled for 30 min under ethanol in an agate mortar. The final powder product was loaded in a gold or platinum capsule and hermetically welded.

Syntheses below 400 MPa and 873 K were carried out in externally heated cold-seal vessels. The experimental set-up is detailed in Ref. [23]. Syntheses at pressures between 400 and 800 MPa, and temperatures above 873 K, were performed in an Edinburgh-type internally heated pressure-vessel (IHPV) using argon as pressure medium. Gas pressure is measured with an electronic gauge to ± 1.5% and temperature was monitored by two S-type $Pt/PtRh_{10}$ thermocouples. Synthesis at pressures from 1 to 4 GPa were carried out in an end-loaded piston-cylinder apparatus (Paris). An encapsulated sample was loaded in a conventional high-pressure assembly consisting of NaCl-sleeves as a pressure transmitting media and a graphite straight-wall furnace; see Ref. [24] for details. Temperature is measured with an S-type $Pt/PtRh_{10}$ thermocouple. Pressure calibration was done by using two known phase equilibria: farringtonite ↔ $Mg_3(PO_4)_2$-II phase transition [25] and albite ⇔ jadeite + quartz reaction [26].

A few syntheses at higher pressures up to 8 GPa were carried out in a multi-anvil MA-8 apparatus [27]. Tungsten carbide cubes with 40-mm edges and 25-mm truncation-edge lengths were used. The pressure medium is a MgO-based octahedron (17-mm edges) with a stepped graphite furnace. For more experimental details, the reader is referred to Ref. [27].

2.2. X-ray diffraction

All run products were first characterised using X-ray powder diffraction. Ten milligrams of the powder sample was ground under ethanol in an agate mortar

and smeared with ethanol on a glass slide. X-ray diffraction patterns were acquired on an INEL diffractometer (CoK_α radiation) equipped with a CPS 120 detector. Silicon (NBS standard) pattern is used to convert channels into diffraction angle ($2\theta°$). Precise lattice parameters of selected single crystals (60–90 μm in average size) have been determined by means of single-crystal diffraction. The unit-cell parameters of the sample crystals were determined using a Huber four-circle diffractometer operated with non-monochromatized Mo X-ray radiation and using a single-point detector. Details of the instrument setting and the peak-centering algorithm are provided in Refs. [28,29]. The effects of crystal offsets and diffractometer aberrations were eliminated by applying the diffracted-beam technique [30]. Lattice parameters determined by a least-squares fit to the corrected setting angles of reflections showed no deviations from symmetry-constrained unit-cell parameters. The values of symmetry-constrained lattice parameters obtained by a vector-least squares fit [31] were determined from 22 to 27 accessible reflections up to 35° in $2\theta°$. When crystal size was not suitable for single-crystal diffraction, lattice constants were refined on powder using the UnitCell software [32].

2.3. High-pressure and high-temperature impedance spectroscopy

Electrical impedance measurements were performed on synthetic $Na_3Al_2(PO_4)_3$ powders at pressures from 0.3 to 1.5 GPa and temperatures up to 1050 K in an end-loaded piston-cylinder press [33] in Frankfurt. The room temperature Bi I–II and Bi II–III transformations at 2.56 and 2.7 GPa [34], respectively, as well as the melting curves of NaCl and CsCl [35] and the $\alpha-\beta$ transition in $LiNaSO_4$ [33] were used for pressure calibration. Melting points of NaCl and CsCl as a function of pressure up to 2.5 GPa have been determined by in-situ electrical conductivity measurements and compared with the table values. Pressure is believed to be accurate within ± 0.05 GPa. Electrical impedance measurements were carried out using a Solartron™ 1260 Phase-Gain-Analyser interfaced with a PC. The device permits a single sine drive and analysis of a system under test over the frequency range of 10 μHz to 32 MHz. In this study, we applied a 1-V sine signal over the frequency range of 0.01 Hz to 100 kHz. Typically, the frequency scan were performed with logarithmic frequency steps of 0.2–0.5 log units. Signals at higher frequencies (>100 kHz) were affected by cable impedance, and at lower frequency (<0.01 Hz) signals became too noisy.

A cell for electrical impedance measurements in the piston cylinder utilised a coaxial cylindrical capacitor with two electrodes from pure Pt-tubes of 0.1 mm in thickness. Both outer and inner electrodes are made from Pt-tube having a diameter of $D=3.8$ mm and $d=2.2$ mm, respectively. The estimated geometric factor G varied from 5.8 to 6.3 cm from one experiment to another. The exact geometric factor of the cell was evaluated independently before high pressure impedance measurements from calibrations on NaCl solutions (for details see Ref. [33]). The starting material in the form of polycrystalline powder was pressed in a coaxial cylindrical gap between the two Pt-electrodes. Measurements of the geometric factor of the cell after high-pressure experiments revealed that due to the cell deformation under pressure the length of the cylindrical capacitor L increases by ~ 3–4%, the outer diameter D increases by 1–2%, and the inner diameter d remains constant. The main advantage of using a coaxial cylindrical geometry instead of a parallel plate geometry in a piston-cylinder apparatus is the negligible change of the geometric factor during loading of the cell under pressure.

During impedance measurements in the piston-cylinder, the press was isolated from the ground of the Solartron™ 1260. Wires from the Pt-thermocouple and the nongrounded mass of the high-pressure autoclave were used to connect the measuring device and the cell electrodes. After each set of measurements, a measuring circuit was calibrated for short-circuit and open-circuit impedance over the frequency range 1 MHz–0.01 Hz. A typical AC-resistance of the cell to a short connection was ~ 0.4 Ω. These calibrations have been taken into account in the final calculations of the electrical impedance as a function of frequency (Novocontrol® software). The electrical impedance measurements were conducted without automatic temperature control in order to avoid the electrical noise from the thyristor regulating the electric power applied to a graphite furnace in the high-pressure assembly. The temperature was adjusted manually through a variable transformer. The hydraulic oil

pressure in the piston ram was regulated by the use of a servo-motor pushing back and forth the piston in a separate hydraulic cylinder. The estimated accuracy of pressure is ± 50 MPa, the accuracy of temperature is ± 3 K.

3. Results

3.1. Syntheses and characterization of quenched products

Three $Na_3Al_2(PO_4)_3$ polymorphs have been identified, named $Na_3Al_2(PO_4)_3$-I, -II and -III hereafter, in dry syntheses performed from ambient pressure up to 8 GPa in the 848–1273 K temperature range (Table 1). Syntheses in the presence of water were avoided since they were found to lead to the formation hydrous aluminium Na-phosphates.

Two experiments have been performed at atmospheric pressure in order to reproduce early results on $Na_3Al_2(PO_4)_3$ compounds from Refs. [22,36]. The $Na_3Al_2(PO_4)_3$ starting material was placed in a platinum crucible and held at 1273 K for 1 or 2 h, and then was either quenched in air (run #1, Table 1) or slowly cooled at a 1 °C/min rate (run #2, Table 1). The diffraction pattern of the run #1 displays the characteristic $AlPO_4$-tridymite reflections along with α-Al_2O_3 (corundum) and a strong amorphous diffusion signal probably due to significant amounts of a sodium-phosphate glass. In run #2, $AlPO_4$ and Al_2O_3 seem to have reacted with the melt component and several additional Bragg's reflections are present on the X-ray pattern which could be attributed neither to the $Na_3Al_2(PO_4)_3$ produced by [36] nor to any known structure.

Table 1
Results of the $Na_3Al_2(PO_4)_3$ syntheses

Run#	Apparatus	T (K)	P (GPa)	Duration	End products
1	AP	1273	Atm.	1 h	$AlPO_4^t$ + Al_2O_3 + amorph.
2	AP	1273	Atm.	1 h	$AlPO_4^t$ + Al_2O_3.+?
4	IHPV	873	0.66	5 days	I + $Na_7(AlP_2O_7)_4PO_4$
5	CSV	873	0.15	17 days	I+?
6	CSV	923	0.1	8 days	I
7	CSV	823	0.4	15 days	I
8	IB	1053	0.18	4 days	I
9	IHPV	923	0.56	6 days	II + I
10	PC	848	0.85	5 days	II
11	PC	848	1.4	5 days	II
12	PC	1073	2.1	33 h	II
13	PC	1273	2.0	4 days	II
14	PC	848	1.7	5 days	II
15	PC	973	2.1	33 h	II
16	PC	973	2.9	96 h	II+?
17	PC	1073	3.9	3 days	III
18	MA	1073	6.0	30 h	III
20	MA	1073	8.0	24 h	III + amorph.

CSV: cold-seal vessel; IB: isochoric bombs; IHPV: internally heated pressure-vessel; PC: piston-cylinder apparatus; amorph.: amorphous material; $AlPO_4^t$: $AlPO_4$ tridymite; "?": unidentified phase(s).

Table 2
Electron microprobe analyses (Cameca SX50) performed on crystals dispersed in epoxy, and calculated structural formulae on a 32-oxygen basis

	I	II	III
	0.18 GPa/780 °C	0.6 GPa/750 °C	3.9 GPa/800 °C
Na_2O	19.2(2.2)	20.1(1.5)	20.2(3.6)
Al_2O_3	24.3(2.7)	24.9(8)	25.0(2.0)
SiO_2	0.3(3)	0.2(1)	0.2(0.3)
P_2O_5	55.0(1.5)	54.4(1.0)	55.9(2.6)
CaO	0.1(1)	0.1(1)	0.1(0.1)
FeO	0.0(0)	0.0(1)	0.0(1)
Σ	99.0(3.6)	99.7(2.0)	101.5(3.0)
32 oxygens			
Na	2.5(3)	2.6(2)	2.6(5)
Al	1.9(2)	2.0(1)	1.9(2)
Si	0.0(0)	0.0(0)	0.0(0)
P	3.1(1)	3.1(1)	3.1(1)
Ca	0.0(0)	0.0(0)	0.0(0)
Fe	0.0(0)	0.0(0)	0.0(0)

The 2σ error is in parentheses. Standards: albite (Na), diopside (Ca, Si), apatite (P), orthoclase (Al), hematite (Fe). Electron beam conditions: 10 nA, 15 kV.

Syntheses at pressures up to 0.66 GPa yielded a first compound with a $Na_3Al_2(PO_4)_3$ composition, $Na_3Al_2(PO_4)_3$-I (see electron microprobe analyses in Table 2). In a run at 660 MPa, 873 K, beside $Na_3Al_2(PO_4)_3$-I, a large amount of $Na_7(AlP_2O_7)_4PO_4$ is present (the corresponding starting mixture has not been further used). It should be noted that most of the $Na_3Al_2(PO_4)_3$-I reflections are also present in the diffraction pattern of $Na_3Al_2(PO_4)_3$ from Ref. [36], which displays additional reflections that could be attributed to $Na_7(AlP_2O_7)_4PO_4$ (Table 3).

Selected crystals from the products of run #7 and #8 were analysed by means of single-crystal X-ray

Table 3
Main $Na_3Al_2(PO_4)_3$-I reflections (highest intensity reflections in bold), comparison to $Na_3Al_2(PO_4)_3$ (JCPDS 31-1265) and tentative indexation using the tetragonal cell inferred from single-crystal experiments

$Na_3Al_2(PO_4)_3$ JCPDS (31-1265)	$Na_3Al_2(PO_4)_3$-I (XRPD)	Tetragonal cell (single-crystal data)
5.16[a,b]	8.38	011
4.65[b]	5.18	103
4.43	4.67	004
4.16	3.48	213
3.87[a]	**3.31**	024
3.74[a]	2.84	–
3.61[a]	2.82	116
3.47[b]	**2.61**	206
3.29[b]	2.59	034
3.13[a]	2.14	136
2.94[a]	2.13	325
2.79[b]	1.80	425

[a] Reflection from $Na_3Al_2(PO_4)_3$-I.
[b] Reflection from $Na_7(AlP_2O_7)_4PO_4$.

diffraction and revealed a strong pseudosymmetry. Most of the crystals are multiply twinned individuals with typical splitting of the Bragg reflections. Only in one case was it possible to derive an orientation matrix for a single domain revealing a (pseudo)tetragonal primitive unit-cell with $a = 9.313(15)$ Å and $c = 18.658(32)$ Å. Remarkably, these lattice parameters indicate pseudocubic symmetry with $c = 2a$. Unfortunately, the crystal was too small (40 μm) for reliable intensity measurements in order to determine both space-group symmetry and structure, and even attempts using a CCD-based detector system failed. Although the powder pattern of the corresponding product could be indexed on the basis of the tetragonal unit-cell (Table 3), both the splitting of reflections and the occurrence of twin-domain reflection sets indicate further symmetry breaking probably due to symmetry-related phase transitions.

Another polymorph, $Na_3Al_2(PO_4)_3$-II, is encountered at higher pressure, between 0.56 and 2.9 GPa. At 0.56 GPa (923 K), both $Na_3Al_2(PO_4)_3$-II and $Na_3Al_2(PO_4)_3$-I coexist in the run product. $Na_3Al_2(PO_4)_3$-II shows a diffraction pattern consistent with a NASICON-type structure. Single-crystal diffraction confirms the rhombohedral NASICON unit-cell with $a = 8.471(4)$ and $c = 21.166(9)$, space group $R\text{-}3c$. Actually, the presence of the 101 reflection in the $Na_3Al_2(PO_4)_3$-II powder pattern precludes the $R\text{-}3c$ (or $R3c$) space-group. It is therefore likely that, like $Na_3Fe_2(PO_4)_3$ [14], only the monoclinic modification of the $Na_3Al_2(PO_4)_3$ NASICON-cell can be quenched.

A third polymorph, $Na_3Al_2(PO_4)_3$-III, was obtained in higher-pressure experiments at 1073 K, 3.9 and 6.0 GPa. The X-ray powder pattern of this latter form (run #17) could be indexed in a $Na_3Fe_2(AsO_4)_3$-II structure with $a = 12.948(5)$, $c = 17.814(11)$. The product recovered after a run at higher pressure (8.0 GPa and 1073 K) appeared to be partly amorphous; $Na_3Al_2(PO_4)_3$-III is present but poorly crystallised.

3.2. Results of high-pressure impedance spectroscopy (HPIS)

HPIS measurements have been performed on both $Na_3Al_2(PO_4)_3$-I and $Na_3Al_2(PO_4)_3$-II. The obtained frequency scans of the measured electrical impedance are presented in a series of Argand plots (Fig. 2). The conductivity scans were fitted to the superposition of two power-law dependencies corresponding to two RC-circuits with a constant phase element [37].

$$\sigma(\omega) = \sigma_0 \times [1 + (j \times \omega \times \tau_0)^n] + \sigma_{DC} \times [1 + (j \times \omega \times \tau_{AC})^p] \quad (1)$$

where the first term is ascribed to the Na^+ blocking response at the surface of the Pt electrodes at low frequencies and the second term is ascribed to the bulk properties of the investigated material at high frequencies [38]. Parameter σ_{DC} represents a bulk DC-conductivity of a sample, p is the frequency exponent varying in the range from 1 to 0. Typical Argand plots of the two polymorphs, $Na_3Al_2(PO_4)_3$-I and $Na_3Al_2(PO_4)_3$-II, are shown in Fig. 2. Parameter σ_{DC} has been estimated from these plots and Eq. (1) for each temperature and pressure. The bulk DC conductivity is a temperature-activated property and is usually found to obey the Arrhenius dependence:

$$\sigma_{DC} \times T = \sigma_0 \times \exp\left(-\frac{E_\sigma}{kT}\right) \quad (2)$$

where σ_0 is the pre-exponential factor and E_σ is the activation energy of the electrical conductivity.

The electrical conductivity properties of $Na_3Al_2(PO_4)_3$-I are presented in the Arrhenius plot in Fig. 3. For comparison, the data for amorphous

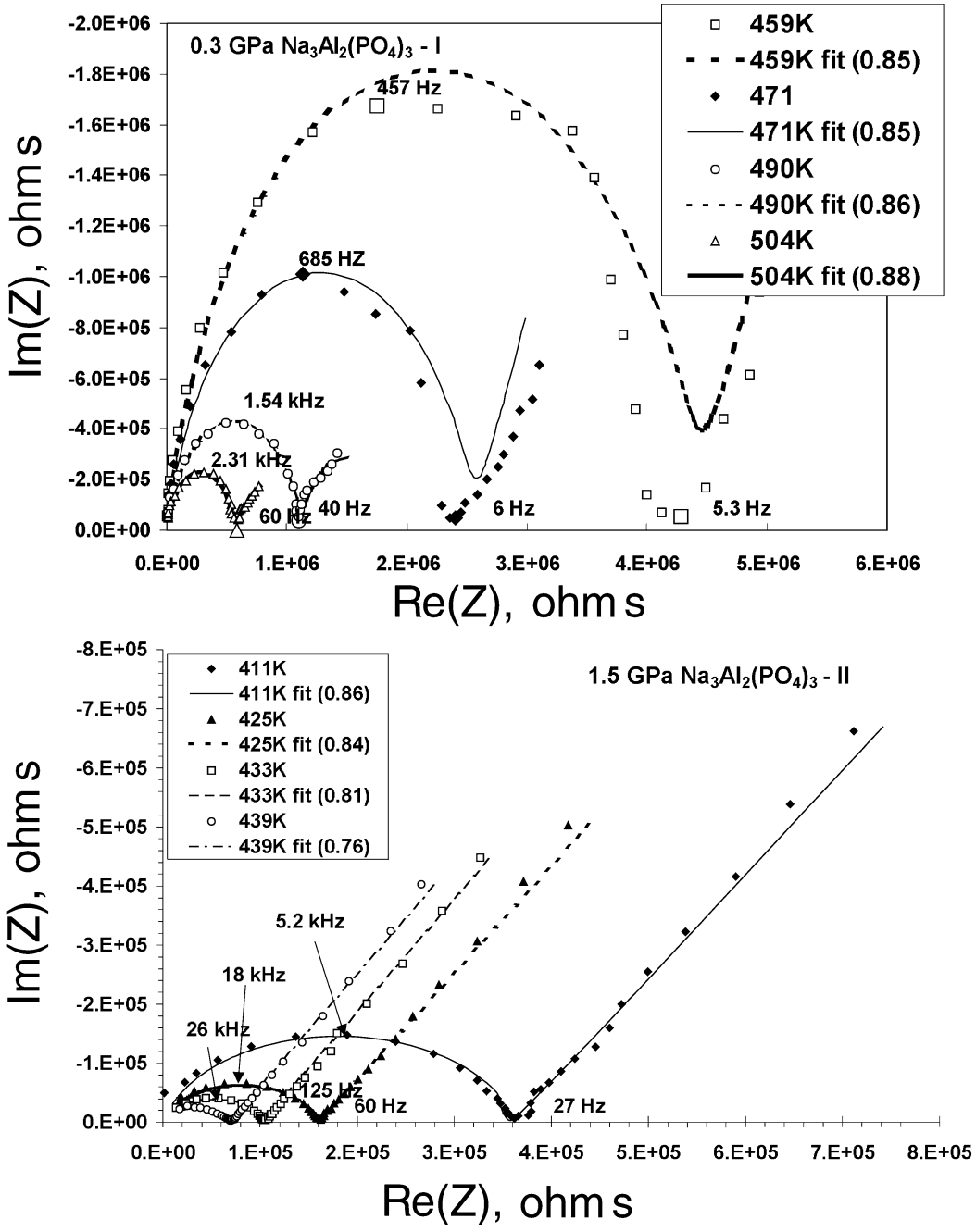

Fig. 2. (Upper panel) Argand plots of $Na_3Al_2(PO_4)_3$-I at pressure 0.3 GPa; geometric factor of the electric cell $G = 6.31$ cm. (Lower panel) Argand plots of $Na_3Al_2(PO_4)_3$-II (monoclinic, α form) at 1.5 GPa; G = 5.74 cm. Numbers in brackets are values of the polarisation exponent p, a fitting parameter in Eq. (1).

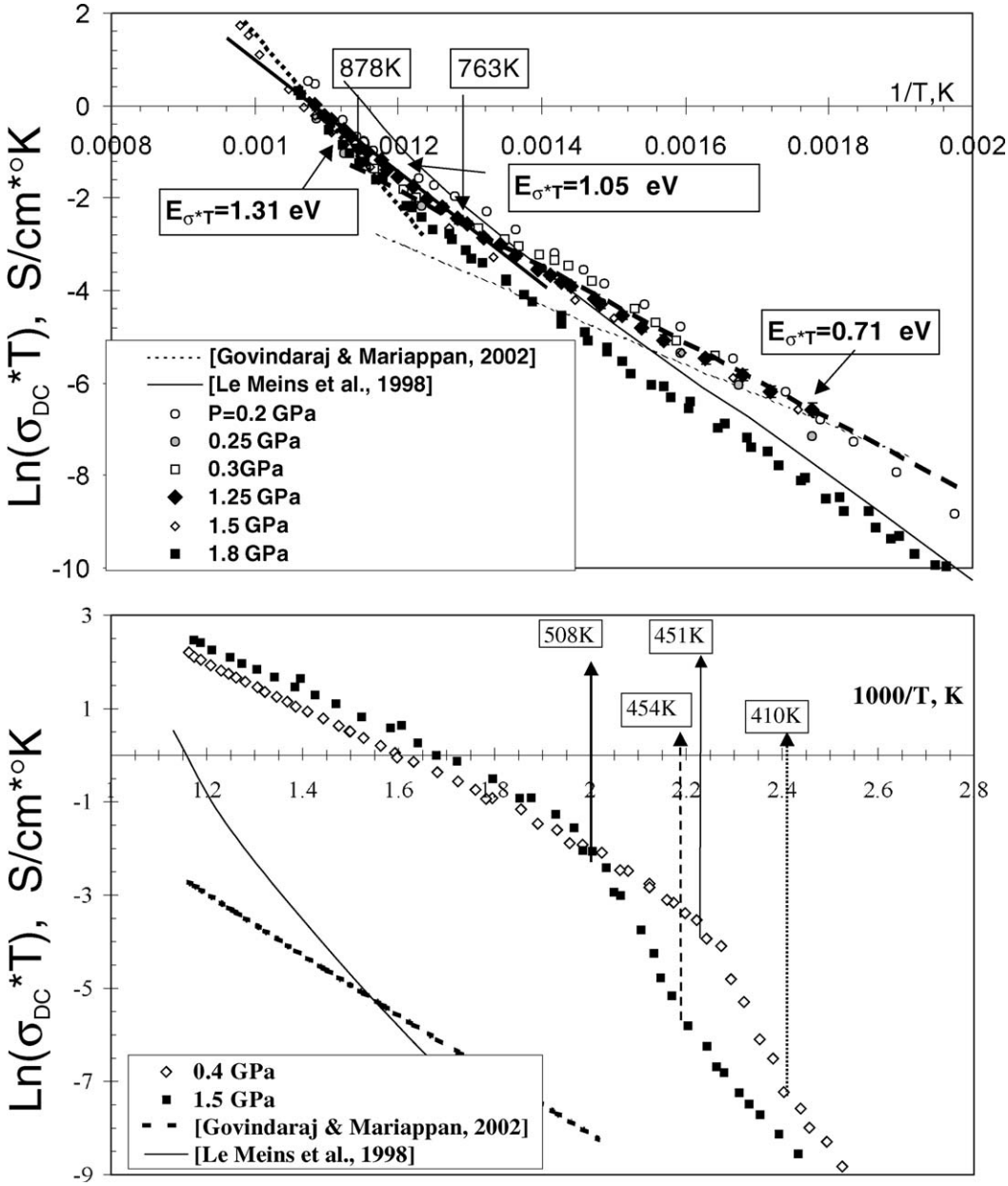

Fig. 3. (Upper panel) Arrhenius plot of the bulk resistance of low pressure polymorph $Na_3Al_2(PO_4)_3$-I at different pressures. At temperatures above ca. 763 K the character of the conductivity changes which is marked by the increase of the activation energy. Extrapolation to this temperature range of the conductivity data of Refs. [38,39] shows that the ionic conductivity of amorphous $Na_3Al_2(PO_4)_3$ and $Na_3Al_2(PO_4)_2F_3$, respectively, are close to that of this polymorph. (Lower panel) Arrhenius plot of $Na_3Al_2(PO_4)_3$-II, polymorph of a crystalline NASICON structure. Two displacive phase-transitions are marked by a change in the activation energy. Conductivity of this polymorph at temperatures above 508 K is 2.5 orders of magnitude higher than the extrapolated data for $Na_3Al_2(PO_4)_3$-glass [39] and non-NASICON structure compound $Na_3Al_2(PO_4)_2F_3$ [38].

$Na_3Al_2(PO_4)_3$ [39] are shown on the same graph. In the 473–873 K temperature range, the real component of the bulk conductivity σ is relatively low, i.e. from 10^{-7} to 10^{-4} S/cm. The temperature dependence of the bulk resistance follows an Arrhenius law with a kink around 763 K at 0.3 GPa. Below 763 K the activation energy of DC conductivity is ~ 0.7 eV. The activation energy slightly varies from 1.05 to 1.31 eV, from 773 to 873 K. These values compare well with results obtained on $Na_3Al_2(PO_4)_2F_3$ E_σ~ 0.8 eV [38] but are definitely higher than those expected for fast sodium conductors. The values of the activation energy estimated from Eq. (2) are listed in Table 3. They are higher than the reported value for $Na_3Al_2(PO_4)_3$ glass 0.5 eV [39]. The increase of the activation energy above 763 K indicates either a new conduction mechanism or an increase of mobile species in the structure which was observed in the compound $Na_3Al_2(PO_4)_2F_3$ [38]. The melting temperature determined from the drop of resistance to ca. 25 Ω cm is about 1153 K at 0.3 GPa. Polarization exponent p in Eq. (1) is smaller than 1. Below 763 K, p is ~ 0.8 and above 763 K, p increases to ~ 1. The physical meaning of $p<1$ is that the hopping motion of Na^+ is translational and involves a big hop [38]. The large value of the activation energy indicates also a nonlocalised motion but rather a macroscopic diffusion of a sodium ion.

The $Na_3Al_2(PO_4)_3$-II polymorph of NASICON structure has been initially synthesised at 1.4 GPa, 848 K (run #11) and was loaded in the HPIS cell and held at 0.4 GPa at room temperature. The first set of measurements was carried out isobarically at 0.4 GPa in the 523–853 K temperature range. The typical scans of the resistivity at low temperatures are shown in Fig. 4 on an Argand plot. The fitting parameters in Eq. (2) vary with temperature from 411 to 439 K: τ_{AC} from 2.9×10^{-5} to 4.9×10^{-6}, and p from 0.86 to 0.76. The bulk DC conductivity of the sample obtained from Eq. (1) is displayed in Fig. 3 (lower panel) at 0.4 and 1.5 GPa, respectively. The first measurements show a high conductivity for a ceramic material consistent with a fast ion conductor material. The data obtained for this first heating stage are rather scattered on the Arrhenius plot. This is the expected behaviour for a powder sample that has not achieved good compaction and sintering. For that reason the sample is held (15 h) at 0.4 GPa and 853 K. Com-

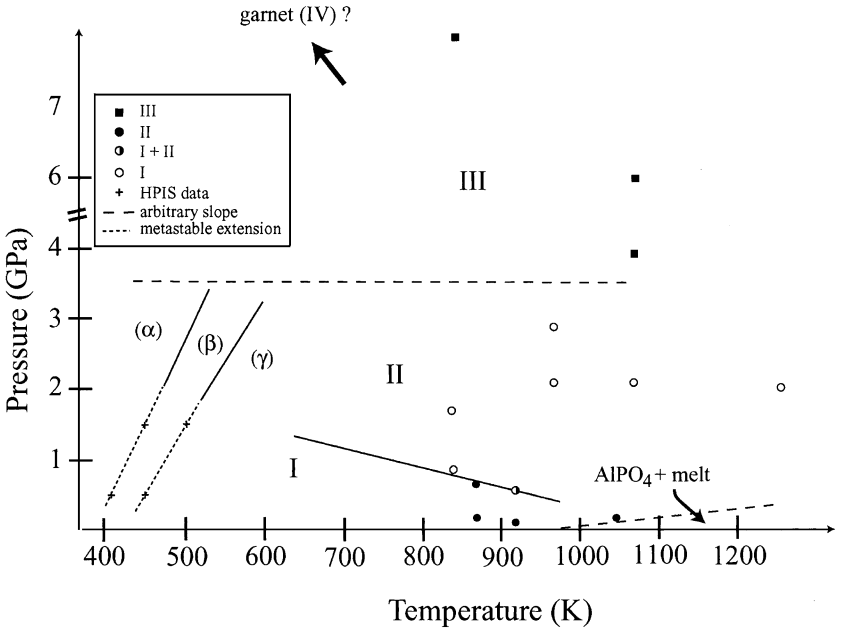

Fig. 4. Tentative $Na_3Al_2(PO_4)_3$ phase diagram based on synthesis experiments and HPIS data. $Na_3Al_2(PO_4)_3$ melting temperature at atmospheric pressure is from Ref. [36]. Melting temperature at higher pressure (0.3 GPa) is estimated from HPIS measurements on $Na_3Al_2(PO_4)_3$-I.

paction and sintering generally lead to a slight resistivity increase.

Upon cooling down to 393 K at an average cooling rate of 1 K min^{-1}, two changes in activation energy are encountered at 451 and 410 K, respectively (Fig. 3, lower panel). These changes are confirmed upon a second heating cycle and are consistent with conductivity measurements carried out on $Na_3Fe_2(PO_4)_3$ NASICON at atmospheric pressure [14].

Pressure is then slowly increased from 0.4 up to 1.5 GPa at 633 K within 30 min. The real component of the electric impedance (Z') at 1 kHz (which approaches the bulk DC impedance value) is found to increase from 830 to 1810 Ω cm (i.e. 890 Ω cm GPa^{-1}). Then, the sample is held overnight at 853 K, 1.5 GPa, i.e. under $P-T$ conditions close to the initial sample synthesis conditions. Sample resistivity is found to decrease from 170 down to 70 Ω cm. It seems, therefore, that the amount of low-pressure phase produced at 0.4 GPa back-transformed into the initial polymorph. It should be noted that due to the presence of $Na_3Al_2(PO_4)_3$-I in the sample measured at 0.4 GPa, sample resistance measured at 1.5 GPa is lower than that measured at 0.4 GPa at the same temperature, contrary to the expected trend for a single-phase material.

Cooling the sample at around 1 K min^{-1} down to 411 K allows to meet the two phase-transitions encountered at 0.4 GPa but shifted to higher temperatures (508 and 454 K). Again, these transitions are fully reversible and confirmed upon heating. X-ray pattern of the recovered material yielded $Na_3Al_2(PO_4)_3$-II plus small amounts of $Na_3Al_2(PO_4)_3$-I. The level of the fast ionic conductivity in $Na_3Al_2(PO_4)_3$-II polymorph is about 2.5 orders of magnitude higher than the extrapolated values for $Na_3Al_2(PO_4)_3$ glass [39]. The activation energy of the bulk DC conductivity is ~0.4 eV, which compares well with the values for other NASICON-type compounds [39,40]. Activation energies of the σ_{DC} of all $Na_3Al_2(PO_4)_3$ phases obtained in this study under pressure are found in Table 4.

Table 4
Activation energies of $\sigma_{DC} \times T$ of $Na_3Al_2(PO_4)_3$ (eV)

Pressure (GPa)	$Na_3Al_2(PO_4)_3$-II, crystalline NASICON structure		
0.4	1.11 ± 0.09	1.7 ± 0.1	0.43 ± 0.06
	(T<410 K)	(410 K<T<451 K)	(451 K<T)
1.1	1.03 ± 0.08	1.5 ± 0.1	0.42 ± 0.07
	(454 K<T)	(454 K<T<508 K)	(508 K<T)
	$Na_3Al_2(PO_4)_3$-I, crystalline non-NASICON structure		
0.3–1.2	0.71 ± 0.06	1.05 ± 0.05	1.32 ± 0.09
	(T<763 K)	(763 K<T<878 K)	(T>878 K)
1.8	0.86 ± 0.05	1.03 ± 0.05	1.6 ± 0.1
	(T<763 K)	(763 K<T<888 K)	(T>888 K)

4. Discussion

4.1. $Na_3Al_2(PO_4)_3$ phase diagram and electrical conductivity

The results of the quenched experiments and of the HPIS measurements are summarized into a tentative phase diagram in Fig. 4.

$Na_3Al_2(PO_4)_3$-I is likely to be the stable form of $Na_3Al_2(PO_4)_3$ at low pressure. It could even be stable down to atmospheric pressure if one assumes the $Na_3Al_2(PO_4)_3$ synthesis of Ref. [36] as a phase mixture including $Na_3Al_2(PO_4)_3$-I (Table 3). The relatively low ionic-conductivity of $Na_3Al_2(PO_4)_3$-I rather suggests that, contrary to the higher pressure polymorphs, $Na_3Al_2(PO_4)_3$-I does not crystallise into a fully open structure. It is therefore an unusual case of structure opening driven by pressure that renders the $Na_3Al_2(PO_4)_3$-I structure determination an exciting issue. The twinning of $Na_3Al_2(PO_4)_3$-I crystals observed in single-crystal diffraction experiments suggests a phase transition that could occur at around 763 K, in the 0.3–1.8 GPa range, according to our HPIS measurements. Submitted to pressure above 0.5 GPa, $Na_3Al_2(PO_4)_3$-I transforms into $Na_3Al_2(PO_4)_3$-II which shows a NASICON structure like other $Na_3(Me^{3+})_2(PO_4)_3$ phosphates. The conductivity mechanism in $Na_3Al_2(PO_4)_3$-I is translational motion of Na^+ ions [38]. The window allowing the translational movement of Na^+ from one structural cavity to another is comparable with the size of the ion. This explains a rather high value of the activation energy of DC bulk conductivity. The requirement of high pressure to stabilise the NASICON structure is in keeping with the small size of the cation found in each $Na_3Al_2(PO_4)_3$ crystallographic site. The molar volume of $Na_3Al_2(PO_4)_3$-II is compared to that of other NASICON compounds, either phosphates (Na- or

Table 5
Volume of selected compounds with a NASICON-type structure

	V/Z (Å^3)		V/Z (Å^3)
$NaCoSc(SO_4)_3$	240.5[a]	$NaNiSc(SO_4)_3$	237.5[a]
$NaMnSc(SO_4)_3$	238[a]	$NaZnSc(SO_4)_3$	239.5[a]
$NaMgSc(SO_4)_3$	238.5[a]	$Sr_{0.5}Hf_2(PO_4)_3$	250.5[b]
$Mg_{0.5}Hf_2(PO_4)_3$	252.5[b]	$Ba_{0.5}Hf_2(PO_4)_3$	255.5[b]
$Ca_{0.5}Hf_2(PO_4)_3$	253.5[b]	$NaZr_2(PO_4)_3$	264.6[c]
$Ca_{0,5}Ti_2(PO_4)_3$	223.3[d]	$NaTi_2(PO_4)_3$	226.7[c]
$Ca_{0,5}Zr_2(PO_4)_3$	256.9[e]	$NaGe_2(PO_4)_3$	204.3[c]
$Li_3Fe_2(PO_4)_3$	259.03[f]	$Na_3Fe_2(PO_4)_3$	239.9[f]
$Na_3Cr_2(PO_4)_3$	235.9[g]	$Na_3Al_2(PO_4)_3$	220.4

[a] [44].
[b] [45].
[c] [10].
[d] [46].
[e] [47].
[f] [14].
[g] [48].

Li-bearing) or sulfates (Table 5). Among the depicted phases, $Na_3Al_2(PO_4)_3$ shows one of the smallest volume and is, to our knowledge, the $X^+{}_3(Y^{3+})_2(Z^{4+}O_4)_3$ NASICON phase with the highest compaction ever reported. Interestingly, $Na_3Al_2(PO_4)_3$-II is super ionic conductor at high pressure with conductivity values around 3×10^{-8} and 5×10^{-2} S/cm at 373 and 973 K, respectively, at 1.5 GPa, i.e. close to that of the best NASICON-type conductors. For comparison, along the NASICON series $Na_{1+x}Zr_2Si_x(P_{1-x/3}O_4)_3$, conductivity varies from 3×10^{-1} S/cm at 773 K to 5×10^{-4} S/cm at 323 K for $x=2$, and from 3×10^{-2} S/cm at 773 K to 4×10^{-4} S/cm at 323 K for $x=1.2$ [41]. In $Na_3Zr_{2-x/4}Si_{2-x}(P_{1+x/3}O_4)_3$, $x=1/3$, conductivity is highest for the compositions of NASICON structure and varies from 2×10^{-2} S/cm at 473 K to 3×10^{-4} S/cm at 303 K [42]. Conductivity of compounds of the $Na_{1+x}Zr_{2-x}In_x(PO_4)_3$ series ($0<x<0.8$) at ambient pressure varies from 10^{-3}–10^{-4} S/cm at 200 °C to 5×10^{-6}–5×10^{-7} S/cm at 303 K [7]. For the $Na_{1.4}Me_{1.6}In_{0.4}(PO_4)_3$ series of NASICON structure with Me = Ti, Sn, Hf, Zr, conductivity ranges from 5×10^{-4} to 5×10^{-3} S/cm at 523 K and from 5×10^{-7} to 5×10^{-5} S/cm at 323 K for Me = Zr and Ti, respectively [3].

In-situ impedance measurements allowed to identify two reversible transitions which have already been reported in similar compounds. By analogy to $Na_3Fe_2(PO_4)_3$, the low temperature phase (i.e. the structure recovered after quenching) corresponds to the α form (monoclinic transformation of the rhombohedral NASICON-cell). The middle- and higher-temperature forms would correspond to β and γ, respectively, two closely related rhombohedral phases of NASICON structure which only show a slight volume difference according to high-temperature diffraction data on $Na_3Fe_2(PO_4)_3$ [14]. A major result of this study is the $Na_3Fe_2(PO_4)_3$-II–$Na_3Fe_2(PO_4)_3$-III transition encountered at pressures above 3 GPa and which involves the transformation of a NASICON structure into another open structure, II-NaFeAs (see Ref. [17] for II-NaFeAs structure description). Again, compared to $Na_3Fe_2(AsO_4)_3$ or $Na_3Cr_2(AsO_4)_3$ of same structure, $Na_3Al_2(PO_4)_3$-III appears to have a volume by around 15% smaller (Table 6).

4.2. Towards a $Na_3Al_2(PO_4)_3$ garnet modification

The stability of a $Na_3Al_2(PO_4)_3$ polymorph with a II-NaFeAs structure is an interesting issue since it renders the existence of $Na_3Al_2(PO_4)_3$ garnet possible. At atmospheric pressure, $Na_3Fe_2(AsO_4)_3$ and $Na_3Cr_2(AsO_4)_3$ show a transition towards low temperatures into a garnet form of smaller molar volume. By analogy, the transformation of $Na_3Al_2(PO_4)_3$-III into a garnet form, if any, is expected at higher pressure (or lower temperature) than that at which $Na_3Al_2(PO_4)_3$-III was obtained. If one applies a volume change of about 9% to 10% at the transition based on the volume change encountered for the arsenate analogues (Table 6), the volume the $Na_3Al_2(PO_4)_3$ garnet (V/Z) would approach is 195 Å^3. The corresponding a-parameter assuming a cubic-garnet cell would then range from 11.5 to 11.6 Å. These predicted values are consistent

Table 6
Expected volume difference (V/Z) between $Na_3Al_2(PO_4)_3$-III and hypothetical $Na_3Al_2(PO_4)_3$-garnet; comparison with $Na_3Cr_2(AsO_4)_3$ and $Na_3Fe_2(AsO_4)_3$ molar volume data

	II-NaFeAs (Å^3)	Garnet (I-NaFeAs)	$\Delta V/V$ (%)
$Na_3Fe_2(AsO_4)_3$	252.6[a]	228.2[a]	−9.6
$Na_3Cr_2(AsO_4)_3$	246.0[b]	223.9[b]	−9.0
$Na_3Al_2(PO_4)_3$	215.5(2)	200.2[c]	−7.1

[a] [49,17].
[b] [49,17].
[c] Calculated volume using the garnet a-parameter obtained from the regression in Ref. [43].

with the 11.7 Å value (i.e. $V/Z \sim 200$ Å^3), calculated using the linear regression in Ref. [43] where the size of the each cation is taken into account (i.e. Na, Al and P).

5. Conclusion

$Na_3Al_2(PO_4)_3$-I, which is likely to be the stable $Na_3Al_2(PO_4)_3$ form at ambient pressure, displays a moderate ionic conductivity comparable to that of amorphous $Na_3Al_2(PO_4)_3$ [39]. Its conductivity increases with temperature due to a progressive opening of the diffusional path of Na in the structure. Due to the relatively small size of the octahedral trivalent cation (i.e. Al^{3+}) in $Na_3Al_2(PO_4)_3$, pressure is required to stabilise the *R*-3*c* NASICON structure for that composition. Application of high pressures on the NASICON polymorph ($Na_3Al_2(PO_4)_3$-II) induces a phase transformation into a NaFeAs-II structure which is also known for its Na-conductivity properties. Towards very high-pressures, above 8 GPa, fast Na-conductivity may cease due to a possible transition into a fourth polymorph with a garnet structure. In addition to the $Na_3Al_2(PO_4)_3$-I structure determination, this study should prompt additional high-pressure and high-temperature investigation towards the suspected garnet field. However, in order to achieve that goal, and due to the now recognised polymorphism wealth in the $Na_3Al_2(PO_4)_3$ system, in-situ characterisation techniques appear as the most appropriate.

Acknowledgements

The authors are grateful to J. Maumus for his help at running the HPIS measurements at IFMG (Frankfurt) and to M.W. Schmidt for the use of the Multi-Anvil apparatus at Clermont-Ferrand (France, INSUE facility). This work was financially supported by Procope and the IT grant 2001/021 (CNRS-INSUE).

References

[1] D. Mazza, J. Solid State Chem. 156 (2001) 154.
[2] O. Bohnke, S. Ronchetti, D. Mazza, Solid State Ionics 122 (1999) 127.
[3] E.R. Losilla, M.A.G. Aranda, S. Bruque, M.A. París, J. Sanz, A.R. West, Chem. Mater. 10 (1998) 665.
[4] W. Bogusz, F. Krok, W. Piszczatowski, Solid State Ionics 119 (1999) 165.
[5] F.E. Mouahid, M. Bettach, M. Zair, P. Maldonado-Manso, S. Bruque, E.R. Losilla, M.A.G. Aranda, J. Mater. Chem. 10 (2000) 2748.
[6] J. Gopalakrishna, K.K. Rangan, Chem. Mater. 4 (1992) 745.
[7] E.R. Losilla, M.A.G. Aranda, S. Bruque, J. Sanz, M.A. París, J. Campo, A.R. West, Chem. Mater. 12 (2000) 2134.
[8] D.A. Woodcock, P. Lightfoot, C. Ritter, Chem. Commun., (1998) 107.
[9] P. Lightfoot, D.A. Woodcock, J.D. Jorgensen, S. Short, Int. J. Inorg. Mater. 1 (1999) 53.
[10] L.O. Hagman, P. Kierkegaard, Acta Chem. Scand. 22 (1968) 1822.
[11] J.M. Winand, A. Rulmond, P. Tartre, J. Solid State Chem. 87 (1990) 83.
[12] G. Collin, R. Comes, J.-P. Boilot, P. Colomban, J. Phys. Chem. Solids 47 (1986) 843.
[13] M. De la Rochère, F. D'Yvoire, G. Collin, R. Comes, J.-P. Boilot, Solid State Ionics 9–10 (1983) 825.
[14] M. Pintard-Scrépel, F. d'Yvoire, F. Rémy, C. R. Acad. Sci., Paris, Sér. C 286 (1978) 381–383.
[15] H.Y.P. Hong, Mater. Res. Bull. 11 (1976) 173.
[16] H. Schwarz, L. Schmidt, Z. Anorg. Allg. Chem. 387 (1972) 31.
[17] F. d'Ivoire, E. Bretey, G. Collin, Solid State Ionics 28–30 (1988) 1259.
[18] S. Khorari, A. Rulmont, P. Tarte, J. Solid State Chem. 134 (1997) 31.
[19] S. Khorari, A. Rulmont, P. Tarte, J. Solid State Chem. 137 (1998) 112.
[20] R.D. Shannon, C.T. Prewitt, Acta Crystallogr., B 25 (1996) 925.
[21] S. Khorari, A. Rulmont, R. Cahay, P. Tarte, J. Solid State Chem. 118 (1995) 267.
[22] E. Thilo, Naturwissenschaften 29 (1941) 239.
[23] F. Brunet, C. Chopin, Contrib. Mineral. Petrol. 121 (1995) 258.
[24] H.J. Massonne, W. Schreyer, Neues Jahrb. Mineral. Abh. 153 (1986) 177.
[25] F. Brunet, D. Vielzeuf, Eur. J. Mineral. 8 (1996) 349.
[26] T.J.B. Holland, Am. Mineral. 65 (1980) 129–134.
[27] M.W. Schmidt, M. Dugagni, G. Artioli, Am. Mineral. 86 (2001) 555.
[28] R.J. Angel, D.R. Allan, R. Miletich, L.W. Finger, J. Appl. Crystallogr. 30 (1997) 461.
[29] R.J. Angel, R.T. Downs, L.W. Finger, in: R.M. Hazen, R.T. Downs (Eds.), High-Temperature and High-Pressure Crystal Chemistry, MSA, Reviews in Mineralogy and Geochemistry vol. 41, 2001, p. 559.
[30] H.E. King, L.W. Finger, J. Appl. Crystallogr. 12 (1979) 374–378.
[31] R.L. Ralph, L.W. Finger, J. Appl. Crystallogr. 15 (1982) 537.
[32] T.J.B. Holland, S.A.T. Redfern, Min. Mag. 61 (1997) 65.

[33] N. Bagdassarov, C.H. Freiheit, A. Putnis, Solid State Ionics 143 (2001) 285.
[34] V.E. Bean, in: G.N. Peggs (Ed.), High Pressure Measurements, Applied Science Publ., London, 1983, p. 93.
[35] S.R. Bohlen, Neues Jahrb. Mineral., Monatsh. H9 (1984) 404.
[36] V.M. Ust'yantsev, L.S. Zholobova, Inorg. Mater. 13 (1977) 1239.
[37] A.K. Jonscher, J. Phys., D. Appl. Phys. 32 (1999) R57.
[38] J.M. Le Meins, O. Bohnke, G. Gourbion, Solid State Ionics 111 (1998) 67.
[39] G. Govindaraj, C.R. Mariappan, Solid State Ionics 147 (2002) 49.
[40] F.E. Mouahid, M. Zahir, P. Maldonado-Manso, S. Bruque, E.R. Losilla, M.A.G. Aranda, A. Rivera, C. Leon, J. Santamaria, J. Mater. Chem. 11 (2001) 3258.
[41] W. Bogusz, F. Krok, W. Piszcatowski, Solid State Ionics 1119 (1999) 165.
[42] O. Bohnke, S. Ronchetti, D. Mazza, Solid State Ionics 122 (1999) 127.
[43] G.A. Novak, G.V. Gibbs, Am. Mineral. 56 (1971) 791.
[44] R. Perret, C. R. Acad. Sci., Paris, Sér. C 280 (1975) 1415.
[45] A.I. Orlova, G.Y. Artem'eva, I.A. Korshunov, N.P. Egorov, Russ. J. Inorg. Chem. 35 (1990) 615.
[46] S. Senbhagaraman, T.N. Guru Row, A.M. Umarji, J. Mater. Chem. 3 (1993) 309.
[47] D.K. Agrawal, V.S. Stubican, Mater. Res. Bull. 20 (1985) 99.
[48] G. Lucazeau, M. Barj, J.-L. Soubeyroux, A.J. Dianoux, C. Delmas, J. Solid State Chem. 18–19 (1986) 959.
[49] F. d'Ivoire, M. Pintard-Screpel, E. Bretey, Solid State Ionics 18–19 (1986) 502.